Letter

# Broadband amplitude squeezing at room temperature in electrically driven quantum dot lasers

Shiyuan Zhao,* Shihao Ding,† Heming Huang, Isabelle Zaquine, and Nicolas Fabre
*LTCI, Télécom Paris, Institut Polytechnique de Paris, 19 Place Marguerite Perey, 91120 Palaiseau, France*

Nadia Belabas
*Université Paris-Saclay, CNRS, Centre de Nanosciences et de Nanotechnologies, 91120 Palaiseau, France*

Frédéric Grillot
*LTCI, Télécom Paris, Institut Polytechnique de Paris, 19 Place Marguerite Perey, 91120 Palaiseau, France*
*and Center for High Technology Materials, University of New Mexico, Albuquerque, New Mexico 87106, USA*

(Received 13 September 2023; revised 18 November 2023; accepted 15 April 2024; published 26 July 2024)

The generation of squeezed states of light lies at the heart of modern photonics-based quantum information technologies. Traditionally, optical nonlinear interactions have been employed to produce squeezed states. However, the harnessing of electrically pumped semiconductor lasers offers distinctive paradigms to achieve enhanced squeezing performance for real-world applications. We present the first evidence that quantum dot lasers enable the realization of broadband amplitude-squeezed states at room temperature across a wide frequency range, spanning from 3 GHz to 12 GHz. Our findings are corroborated by a stochastic simulation in agreement with the experimental data.

DOI: 10.1103/PhysRevResearch.6.L032021

The evolution of photonics-based quantum information technologies is currently on the brink of initiating a revolutionary transformation in data processing and communication protocols [1]. A cornerstone within this realm will be the quantum emitter. Over the past years, squeezed states of light have been frequently generated using $\chi^{(2)}$ or $\chi^{(3)}$ nonlinear interactions via parametric down conversion and four-wave mixing [2]. A variety of nonlinear materials have been applied in these processes, including $LiNbO_3$ (PPLN) [3], $KTiOPO_4$ (PPKTP) [4], silicon [5], atomic vapor [6], disk resonator [7], and $Si_3N_4$ [8]. Recent advancements have also facilitated the transition from traditional benchtop instruments to a more compact chip design [9–13]. As opposed to that, Golubev and Sokolov initially introduced the concept of suppressing the statistical nature of the laser pumping process [14]. Later, Yamamoto and colleagues [15] proposed an alternative method to directly produce amplitude-squeezed states with off-the-shelf semiconductor lasers using a "quiet" pump, i.e., a constant-current source. These states are commonly referred to as photon-number squeezed states, which exhibit reduced fluctuations in photon number $\langle \Delta \hat{n}^2 \rangle < \langle \hat{n} \rangle$ compared to coherent states [16], albeit encountering enhanced phase fluctuations due to the minimum-uncertainty principle. A striking peculiarity of semiconductor lasers is their ability to be pumped by injection current supplied via an electrical circuit. Unlike optical pumping, electrical pumping is not inherently a Poisson point process due to the Coulomb interaction and allows for reducing pump noise below the shot noise level [15]. Notably, this method can take full advantage of the mature fabrication processes in the semiconductor industry, thereby significantly boosting its feasibility. While subsequent experiments involving various types of laser diodes have gained widespread interest in this domain, including commercial quantum well (QW) lasers [17,18], vertical-cavity surface-emitting lasers [19], and semiconductor microcavity lasers [20], the observed sub-shot-noise electrical bandwidth has, until now, remained relatively limited. The broadest achieved bandwidth has reached 1.1 GHz with a QW transverse junction stripe laser at a cryogenic temperature of 77 K [21]. Quantum dot (QD) lasers, departing from the conventional QW active region, achieve ultimate quantization through three-dimensional spatial confinement, leading to unparalleled quantum advantage [22]. For instance, self-assembled QDs embedded into microcavities can facilitate the generation of single photons with high purity and indistinguishability [23–25].

In this Letter, we unveil experimental evidence of generating broadband amplitude-squeezed states from a QD semiconductor laser chip at room temperature. Our results confirm that a constant-current-driven QD laser can generate sub-Poissonian light with an extended electrical bandwidth of 9 GHz. This outcome closely aligns with Yamamoto's model [15], which suggests that the intensity noise of the laser output field, rather than the internal field, may be diminished below the shot noise level at the high pump current. To

*shiyuan.zhao@telecom-paris.fr
†shihao.ding@telecom-paris.fr

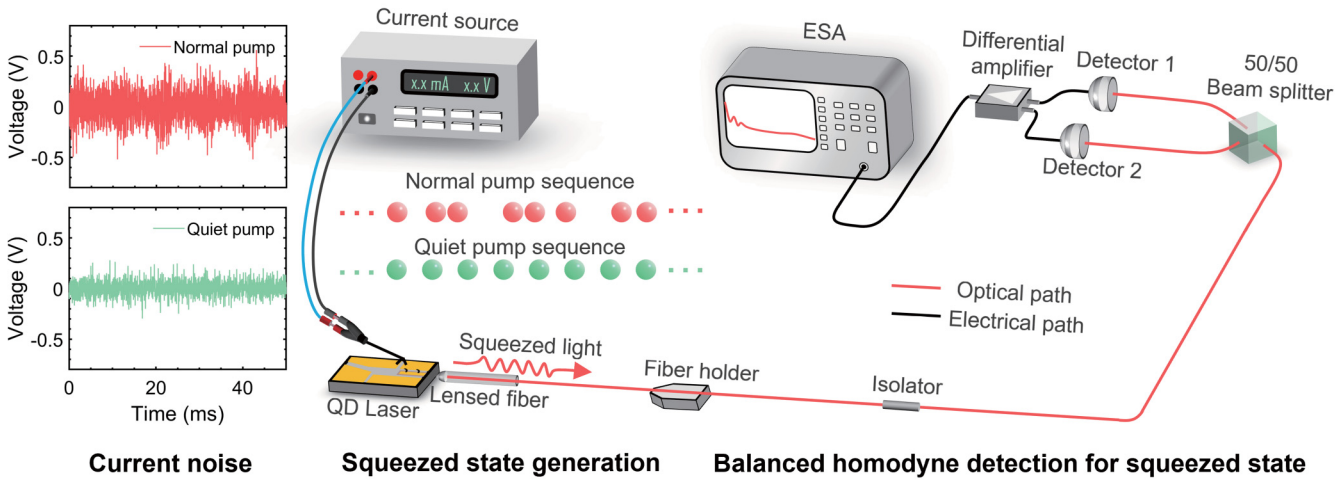


FIG. 1. Diagram of the key components of the apparatus used for generating amplitude-squeezed states through QD lasers. Left panel: Comparison of noise characteristics between two different current sources, namely Keithley 2400 (normal pump, red) and ILX Lightwave LDX-3620 (quiet pump, green). The current noises are assessed by detecting voltage fluctuations across a 10 Ω resistor. Further details can be found in the Supplemental Material [31]. Right panel: Experimental setup. The quiet pump injects electrons at a constant rate and ESA is the electrical spectrum analyzer.

eliminate pump noise, we implemented the high-impedance configuration to achieve uniform regulation of the pumping electrons [15] and accurately characterized the current source noise. Moreover, we have corroborated our findings through numerical simulations using a stochastic algorithm, which complements Yamamoto's model [15] with additional information on photon statistics.

A diagram of the experimental setup is illustrated in Fig. 1. A 1308 nm distributed-feedback (DFB) QD laser is utilized, which features a highly reflective (HR) coating (95%) on the rear facet and an antireflection (AR) coating (3%) on the front facet. To maintain a stable temperature of 20 °C ± 0.005 °C, we use a thermoelectric temperature controller (ILX Lightwave LDT-5748). The QD laser's threshold current $I_{th}$ is measured to be 9 mA. The optical losses degrade the regularity of the photon flux and decrease the squeezing level [21]. We measure a detection efficiency of 55% and a collection efficiency of 40% because of the losses during laser-fiber coupling. Consequently, the overall efficiency is estimated at 22%. Nevertheless, this does not impact the internal quantum efficiency that remains close to unity and pertains to the conversion from injected electrons to emitted photons. The stable single-longitudinal-mode operation is realized over a wide pump current range and the side mode suppression rejection (SMSR) is more than 50 dB at the high pump currents to avoid the side-mode-competition interference [26].

Amplitude-squeezed states demonstrate sub-Poissonian photon statistics, photon antibunching, and squeezing owing to the reduced uncertainty in the photon number [27]. Therefore, we employ a standard balanced homodyne detection for the squeezing measurement [28]. During the measurement process, a DFB QD laser is coupled into a fiber holder and precisely driven by a low-noise current source (ILX Lightwave LDX-3620). The current leaking around the gain medium, rather than flowing into it, does not disrupt the regular flow of electrons from the pump current [29]. A 30 dB optical isolator is imperative because even a minimal amount of back-reflected light leads to excessive intensity noise. After passing through the optical isolator, the output beam is split into two separate paths by a tunable beamsplitter to ensure 50/50 optical balancing. These paths are then detected by two identical photodiodes (discovery semiconductors DSC-R405ER 20 GHz linear balanced photoreceivers). We carefully avoid the detector saturation at the large optical power. The difference between the photocurrent fluctuations is amplified by a homemade low-noise electronic amplifier and subsequently assessed with an electrical spectrum analyzer (ESA) (Rohde and Schwarz, 43 GHz) to obtain the radio frequency (RF) noise power spectral density. Through this balanced detection, excessive intensity noise can be substantially suppressed compared to single photodiode detection. The common-mode rejection ratio (CMRR) consistently exceeds 30 dB across the entire frequency spectrum up to 18 GHz.

Accurate calibration of the shot noise level, also known as the standard quantum limit (SQL), holds paramount importance in this experiment since it serves as a normalization parameter for quantifying the squeezing. In this work, we not only calibrate the SQL using either a filtered incandescent lamp or a semiconductor optical amplifier operating at the same wavelength [21], but also adhere to the original setup while replacing the low-noise current source with the normal pump source (Keithley 2400) [30]. In all measurements, the RF noise power spectral density of the subtracted photocurrent remains consistent, irrespective of alterations in the pump current.

Figure 2(a) depicts the measured RF noise power spectral density for the QD laser biased at 40 mA, illustrating amplitude squeezing (green curve) in comparison to the calibrated SQL (red dashed curve). Within the frequency range of 3 GHz to 12 GHz, there is a significant noise reduction observed below the SQL. The largest noise reduction is 0.9 dB at 8 GHz and it reaches 3.1 dB at the laser output facet after

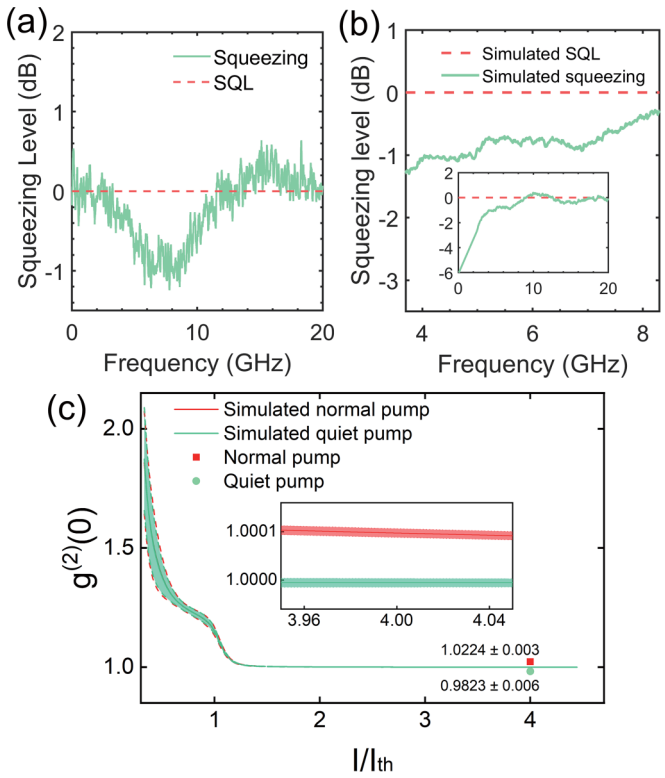


FIG. 2. (a) The measured RF noise power spectral density at 40 mA is represented by the green line (amplitude squeezing). The spectrum analyzer was set to a resolution bandwidth (RBW) of 200 kHz and a video bandwidth (VBW) of 500 Hz. All traces have been corrected for thermal background noise subtraction. (b) The stimulated RF noise power spectral density is shown in green, while the stimulated SQL is represented in the red dashed line. (c) The stimulated normalized second-order correlation function at zero delay $g^{(2)}(0)$ as a function of pump current. The green and red areas show the standard deviation from the average obtained from 100 simulation runs. Two experimental data points are also presented.

correcting for the overall efficiency (see the Supplemental Material) [31,32]. The squeezing electrical bandwidth discussed here surpasses the cutoff frequency of flicker (1/f) noise. Additionally, at such a high pump rate, the relaxation oscillation resonance is effectively suppressed. To further verify this, we redirect our attention to photon statistics to offer further evidence of the amplitude squeezing.

An essential feature of a QD laser with a constant-current source is its inherent capability to directly convert sub-Poissonian statistics of electrons into nonclassical photon statistics. To fully comprehend the underlying mechanisms such as carrier scattering and light-matter interaction, we introduce a set of coupled stochastic differential equations that are adeptly tailored to the three-energy-level QD model [33]:

$$\frac{dN^{RS}}{dt} = R_{\text{pump}} + R_{ES\to RS} - R_{RS\to ES} - R^{RS}_{\text{decay}}, \tag{1}$$

$$\frac{dN^{ES}}{dt} = R_{RS\to ES} + R_{GS\to ES} - R_{ES\to RS} - R_{ES\to GS} - R^{ES}_{\text{decay}}, \tag{2}$$

$$\frac{dN^{GS}}{dt} = R_{ES\to GS} - R_{GS\to ES} - R_{\text{stim}} - R^{GS}_{\text{decay}}, \tag{3}$$

$$\frac{dS^{GS}}{dt} = R_{\text{stim}} - R_{\text{internal}} - R_{\text{mirror}} + R_{\text{spon}}, \tag{4}$$

where $N^i$ (i = RS, ES, GS) represents the carrier density in the reservoir states (RS), excited states (ES), and ground states (GS), respectively. $S^{GS}$ denotes the photon density in the GS, $R^i_{\text{decay}}$ (i = RS, ES, GS) represents the spontaneous emission rate that reduces the carrier density in each energy state. $R_{ES\to RS}$ and $R_{RS\to ES}$ describe the carrier scattering rates between RS and ES, while $R_{ES\to GS}$ and $R_{GS\to ES}$ are the same between ES and GS. $R_{\text{stim}}$ accounts for the stimulated emission rate solely on GS, and $R_{\text{spon}}$ represents the fraction of the spontaneous emission coupled into the lasing mode. Furthermore, the sum of $R_{\text{internal}}$ and $R_{\text{mirror}}$ constitutes the photon decay rate, with $R_{\text{mirror}}$ the outcoupling rate through facet mirrors into the output channel and $R_{\text{internal}}$ containing other internal optical losses. The definitions of the quantities appearing on the right-hand side of Eqs. (1)–(4) and their corresponding parameters are provided in the Supplemental Material [31]. The stimulated RF noise power spectral density is outlined in Fig. 2(b). In this approach, we derive the SQL and the amplitude squeezing independently for normal pumping and quiet pumping conditions by applying Fourier transforms of the time traces. Although an evident squeezing phenomenon can be theoretically anticipated at low frequencies, it is often overshadowed by technical noise in practical settings [21]. Nonetheless, in both the experiments and the simulations, a discernible signature of the amplitude squeezing is observed at relatively high frequencies. In addition, we computed the normalized second-order correlation at zero delay $g^{(2)}(0)$, as depicted in Fig. 2(c), using the simulation data. Following the relationship $\langle \Delta S^2 \rangle = [g^{(2)}(0) - 1]\langle S \rangle^2 + \langle S \rangle$ [30], with $S$ representing the external photon number, we observed that stimulated $g^{(2)}(0)$ rapidly converges to approximately one shortly after passing the laser threshold $I_{th}$. However, under normal pump conditions, $g^{(2)}(0)$ slightly exceeds one at $4 \times I_{th}$, whereas with the quiet pump, $g^{(2)}(0)$ dips just below unity at $4 \times I_{th}$ due to the relatively high average photon number [34]. We also performed corresponding measurements of $g^{(2)}(0)$ at 40 mA, and the experimental results are indicated by two symbols within the same figure, supporting our simulation findings. A recent theoretical study has affirmed that a single-mode Gaussian state can exhibit a $g^{(2)}(0) < 1$ [35]. The spectral distribution of the optical field is observed to be centered around 1308.5 nm in the experiment (see the Supplemental Material [31]). Additionally, the contribution of thermal photons is found to be negligible at room temperature, and hence we obtain a first signature of a displaced squeezed state. This observation will be unambiguously verified through further investigations, involving the full reconstruction of the Wigner function using quantum tomography [36,37].

Figure 3 provides a comparison between measured and simulated photon statistics. The photon number distributions are extracted from experimental data recorded by the oscilloscope and from stochastic simulations. In both scenarios, the histogram for shot noise confirms a Poissonian distribution.

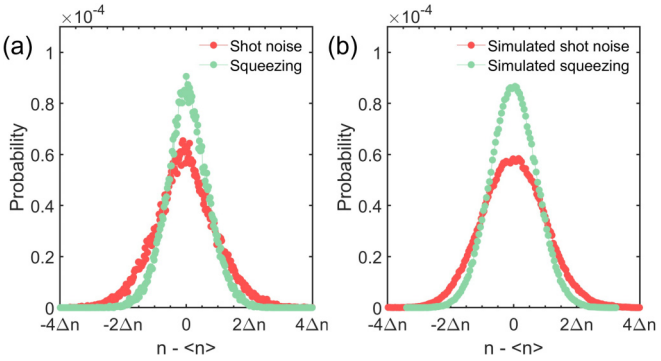


FIG. 3. (a) Histogram calculated from the raw data acquired by the oscilloscope. Each time trace is averaged over five frames and the sampling rate is 20 Gbps. (b) Histogram computed from the simulation data, where each time trace has $2\times10^6$ data points, spanning a time period of 1 μs.

However, under quiet pumping conditions, the distribution becomes narrower, exhibiting sub-Poissonian characteristics that are confirmed by the measurement of the $g^2(0)$ below one.

Yamamoto *et al.* envisaged that a single-mode semiconductor laser with a high internal quantum efficiency could manifest a broad squeezing electrical bandwidth, typically exceeding 100 GHz, ultimately determined by the semiconductor laser photon lifetime ($\tau_p \sim 1$ ps) [15]. However, merely relying on a constant-current source does not unambiguously dictate an anticorrelation between successive injection events into the active layer. This is because each carrier injection constitutes a (Poisson) random point process, driven solely by the junction voltage and the junction's temperature [34]. Nevertheless, it should be underlined that the Coulomb blockade effect can influence the injection rate. For example, the injection of a carrier results in a reduction of the junction voltage by $e/C_{\mathrm{dep}}$, where $C_{\mathrm{dep}}$ represents the depletion layer capacitance. This voltage reduction accordingly leads to a decrease in the carrier injection rate, establishing a negative feedback mechanism that suppresses noise in the carrier injection process. This mechanism operates successfully in the single-photon turnstile device within the mesoscopic domain [23] at low temperatures. But in the macroscopic high-temperature regime, $N = (\frac{k_BT}{e})/(\frac{e}{C_{\mathrm{dep}}}) = k_BTC_{\mathrm{dep}}/e^2$ electrons lead to a substantial junction voltage reduction equivalent to the thermal voltage $k_BT/e$, resulting in the pronounced regulation of the carrier injection rate. Considering that electrons are provided by the current source at a rate of $I/e$, the time required for $N$ electrons to be delivered is $\tau_{te} = k_BTC_{\mathrm{dep}}/eI$. Therefore, this collective behavior of numerous electrons introduces an additional limitation to the squeezing electrical bandwidth $B$ [34]:

$$B = \frac{1}{2\pi(\tau_{te} + \tau_p)} = \frac{1}{2\pi\left(\frac{k_BTC_{\mathrm{dep}}}{eI} + \tau_p\right)}. \tag{5}$$

The squeezing electrical bandwidth is expected to be directly proportional to the current $I$, but inversely proportional to the temperature $T$ and the capacitance $C_{\mathrm{dep}}$. With the specific numerical parameters outlined in Ref. [29], where the depletion layer capacitance of the QW laser is around 280 pF, the calculated squeezing electrical bandwidth is estimated to be around 1 GHz at 66 K. Meanwhile, QD lasers generally feature lower values of $C_{\mathrm{dep}}$, sometimes as low as 3.5 pF [38]. In contrast to QW lasers, this gives rise to a scenario where $\tau_{te} \ll \tau_p$, resulting in a calculated squeezing electrical bandwidth of several tens of gigahertz at room temperature, given that $\tau_p$ in QD lasers is in the order of a few picoseconds [33]. This phenomenon, where the bandwidth in Eq. (5) is only determined by $\tau_p$, is seldom encountered in other types of lasers.

In conclusion, our work has achieved a significant milestone by successfully generating broadband amplitude-squeezed states at room temperature using a constant-current-driven QD laser. This demonstration provides access to a regime where the squeezing electrical bandwidth is dictated by the photon lifetime of the semiconductor laser. The RF noise power spectral density in homodyne detection has been decreased by as much as 0.9 dB (3.1 dB after the correction) across a wide frequency range of 3 GHz to 12 GHz in comparison to the shot noise level. We estimate, by tracking photon losses within our experimental setup, that utilizing direct light collection, fused fibers, and pigtailing could bridge the gap between the observed squeezing level at the spectrum analyzer and the corrected squeezing level at the laser output facet. Achieving higher squeezing levels, however, would necessitate significant engineering advancements in laser cavity design [39,40], external stabilization techniques [17,18], and the ambitious ongoing integration of the entire system onto a single chip, which, nonetheless, appears realistic [11,41]. In our upcoming research, we plan to increase the squeezing level beyond 10 dB using quantum dot technology, focusing on related applications in quantum sensing. Moreover, in practical scenarios, 3–6 dB of squeezing has proven sufficient to outperform coherent states in quantum communication [42,43]. This squeezing level is particularly effective in mitigating the impact of channel noise, such as that induced by atmospheric turbulence in free-space transmission, which could otherwise compromise the rate of secret key exchange [44]. Our results carry direct implications for various quantum information applications, especially in the continuous-variable quantum key distribution (CV QKD) over free-space channels. Bright squeezed semiconductor lasers, as proposed in Ref. [45], offer excellent light sources in this context. For further insights into a simplified CV QKD configuration, please refer to the Supplemental Material [31]. Lastly, we firmly believe that this technology represents a significant stride toward quantum super-resolution imaging, effectively reducing imaging measurement errors in comparison to classical coherent state imaging with the same number of photons [46].

*Acknowledgments.* S.Z. and S.D. contributed equally to this work and jointly conceptualized the work; S.Z. conducted the simulation, and S.D. conducted the experiments. The technical contributions of Prof. W. Elsäßer and Prof. G. Moody are gratefully acknowledged. The authors acknowledge the financial support of the Institut Mines-Télécom and the Air Force Office of Scientific Research (AFSOR) under Grant No. FA8655-23-1-7050. S.D. is also supported by the China Scholarship Council (CSC).

[1] E. Pelucchi, G. Fagas, I. Aharonovich, D. Englund, E. Figueroa, Q. Gong, H. Hannes, J. Liu, C.-Y. Lu, N. Matsuda *et al.*, The potential and global outlook of integrated photonics for quantum technologies, Nat. Rev. Phys. **4**, 194 (2022).

[2] R. E. Slusher, L. W. Hollberg, B. Yurke, J. C. Mertz, and J. F. Valley, Observation of squeezed states generated by four-wave mixing in an optical cavity, Phys. Rev. Lett. **55**, 2409 (1985); L.-A. Wu, H. J. Kimble, J. L. Hall, and H. Wu, Generation of squeezed states by parametric down conversion, *ibid.* **57**, 2520 (1986).

[3] T. Kashiwazaki, T. Yamashima, K. Enbutsu, T. Kazama, A. Inoue, K. Fukui, M. Endo, T. Umeki, and A. Furusawa, Over-8-dB squeezed light generation by a broadband waveguide optical parametric amplifier toward fault-tolerant ultrafast quantum computers, Appl. Phys. Lett. **122**, 234003 (2023).

[4] H. Vahlbruch, M. Mehmet, K. Danzmann, and R. Schnabel, Detection of 15 dB squeezed states of light and their application for the absolute calibration of photoelectric quantum efficiency, Phys. Rev. Lett. **117**, 110801 (2016).

[5] A. H. Safavi-Naeini, S. Gröblacher, J. T. Hill, J. Chan, M. Aspelmeyer, and O. Painter, Squeezed light from a silicon micromechanical resonator, Nature (London) **500**, 185 (2013).

[6] C. McCormick, V. Boyer, E. Arimondo, and P. Lett, Strong relative intensity squeezing by four-wave mixing in rubidium vapor, Opt. Lett. **32**, 178 (2007).

[7] J. U. Fürst, D. V. Strekalov, D. Elser, A. Aiello, U. L. Andersen, C. Marquardt, and G. Leuchs, Quantum light from a whispering-gallery-mode disk resonator, Phys. Rev. Lett. **106**, 113901 (2011).

[8] Y. Zhao, Y. Okawachi, J. K. Jang, X. Ji, M. Lipson, and A. L. Gaeta, Near-degenerate quadrature-squeezed vacuum generation on a silicon-nitride chip, Phys. Rev. Lett. **124**, 193601 (2020).

[9] A. Dutt, K. Luke, S. Manipatruni, A. L. Gaeta, P. Nussenzveig, and M. Lipson, On-chip optical squeezing, Phys. Rev. Appl. **3**, 044005 (2015).

[10] F. Mondain, T. Lunghi, A. Zavatta, E. Gouzien, F. Doutre, M. D. Micheli, S. Tanzilli, and V. D'Auria, Chip-based squeezing at a telecom wavelength, Photonics Res. **7**, A36 (2019).

[11] G. Moody, L. Chang, T. J. Steiner, and J. E. Bowers, Chip-scale nonlinear photonics for quantum light generation, AVS Quantum Sci. **2**, 041702 (2020).

[12] Z. Yang, M. Jahanbozorgi, D. Jeong, S. Sun, O. Pfister, H. Lee, and X. Yi, A squeezed quantum microcomb on a chip, Nat. Commun. **12**, 4781 (2021).

[13] R. Nehra, R. Sekine, L. Ledezma, Q. Guo, R. M. Gray, A. Roy, and A. Marandi, Few-cycle vacuum squeezing in nanophotonics, Science **377**, 1333 (2022).

[14] Y. M. Golubev and I. V. Sokolov, Photon antibunching in a coherent light source and suppression of the photorecording noise, Zh. Eksp. Teor. Fiz. **87**, 408 (1984) [Sov. Phys. JETP **60**, 234 (1984)].

[15] Y. Yamamoto, S. Machida, and O. Nilsson, Amplitude squeezing in a pump-noise-suppressed laser oscillator, Phys. Rev. A **34**, 4025 (1986); S. Machida, Y. Yamamoto, and Y. Itaya, Observation of amplitude squeezing in a constant-current–driven semiconductor laser, Phys. Rev. Lett. **58**, 1000 (1987).

[16] R. J. Glauber, Coherent and incoherent states of the radiation field, Phys. Rev. **131**, 2766 (1963).

[17] H. Wang, M. J. Freeman, and D. G. Steel, Squeezed light from injection-locked quantum well lasers, Phys. Rev. Lett. **71**, 3951 (1993).

[18] J. Kitching, A. Yariv, and Y. Shevy, Room temperature generation of amplitude squeezed light from a semiconductor laser with weak optical feedback, Phys. Rev. Lett. **74**, 3372 (1995).

[19] J. Kaiser, C. Degen, and W. Elsässer, Amplitude-squeezed emission from a transverse single-mode vertical-cavity surface-emitting laser with weakly anticorrelated polarization modes, Opt. Lett. **26**, 1720 (2001).

[20] W. Choi, J.-H. Lee, K. An, C. Fang-Yen, R. R. Dasari, and M. S. Feld, Observation of sub-poisson photon statistics in the cavity-QED microlaser, Phys. Rev. Lett. **96**, 093603 (2006).

[21] S. Machida and Y. Yamamoto, Ultrabroadband amplitude squeezing in a semiconductor laser, Phys. Rev. Lett. **60**, 792 (1988).

[22] F. Grillot, J. Duan, B. Dong, and H. Huang, Uncovering recent progress in nanostructured light-emitters for information and communication technologies, Light: Sci. Appl. **10**, 156 (2021).

[23] P. Michler, A. Kiraz, C. Becher, W. V. Schoenfeld, P. M. Petroff, L. Zhang, E. Hu, and A. Imamoglu, A quantum dot single-photon turnstile device, Science **290**, 2282 (2000).

[24] N. Somaschi, V. Giesz, L. De Santis, J. Loredo, M. P. Almeida, G. Hornecker, S. L. Portalupi, T. Grange, C. Anton, J. Demory *et al.*, Near-optimal single-photon sources in the solid state, Nat. Photon. **10**, 340 (2016).

[25] Y. Arakawa and M. J. Holmes, Progress in quantum-dot single photon sources for quantum information technologies: A broad spectrum overview, Appl. Phys. Rev. **7**, 021309 (2020).

[26] F. Marin, A. Bramati, E. Giacobino, T. C. Zhang, J. P. Poizat, J. F. Roch, and P. Grangier, Squeezing and intermode correlations in laser diodes, Phys. Rev. Lett. **75**, 4606 (1995).

[27] M. Kitagawa and Y. Yamamoto, Number-phase minimum-uncertainty state with reduced number uncertainty in a Kerr nonlinear interferometer, Phys. Rev. A **34**, 3974 (1986).

[28] H. P. Yuen and V. W. S. Chan, Noise in homodyne and heterodyne detection, Opt. Lett. **8**, 177 (1983).

[29] W. H. Richardson, S. Machida, and Y. Yamamoto, Squeezed photon-number noise and sub-Poissonian electrical partition noise in a semiconductor laser, Phys. Rev. Lett. **66**, 2867 (1991).

[30] J. Mørk and K. Yvind, Squeezing of intensity noise in nanolasers and nanoleds with extreme dielectric confinement, Optica **7**, 1641 (2020).

[31] See Supplemental Material at http://link.aps.org/supplemental/10.1103/PhysRevResearch.6.L032021 for details of the squeezing experiments and analysis, our stochastic simulation and a discussion on the influence of quantum information.

[32] A. I. Lvovsky, Squeezed light, in *Photonics: Scientific Foundations, Technology and Applications*, edited by D. L. Andrews (John Wiley & Sons, Ltd, 2015), Chap. 5, pp. 121–163.

[33] C. Wang, M. Osinski, J. Even, and F. Grillot, Phase-amplitude coupling characteristics in directly modulated quantum dot lasers, Appl. Phys. Lett. **105**, 221114 (2014).

[34] A. Imamoglu and Y. Yamamoto, Noise suppression in semiconductor *p-i-n* junctions: Transition from macroscopic squeezing to mesoscopic Coulomb blockade of electron emission processes, Phys. Rev. Lett. **70**, 3327 (1993).

[35] S. Olivares, S. Cialdi, and M. G. A. Paris, Homodyning the $g^{(2)}(0)$ of Gaussian states, Opt. Commun. **426**, 547 (2018).

[36] D. T. Smithey, M. Beck, M. G. Raymer, and A. Faridani, Measurement of the Wigner distribution and the density matrix of a light mode using optical homodyne tomography: Application to squeezed states and the vacuum, Phys. Rev. Lett. **70**, 1244 (1993).

[37] A. Zavatta, F. Marin, and G. Giacomelli, Quantum-state reconstruction of a squeezed laser field by self-homodyne tomography, Phys. Rev. A **66**, 043805 (2002).

[38] D. Inoue, D. Jung, J. Norman, Y. Wan, N. Nishiyama, S. Arai, A. C. Gossard, and J. E. Bowers, Directly modulated 1.3 μm quantum dot lasers epitaxially grown on silicon, Opt. Express **26**, 7022 (2018).

[39] L. A. Ostrowski, T. J. Baker, S. N. Saadatmand, and H. M. Wiseman, No tradeoff between coherence and sub-Poissonianity for Heisenberg-limited lasers, Phys. Rev. Lett. **130**, 183602 (2023).

[40] L. Nguyen, J. Sloan, N. Rivera, and M. Soljačić, Intense squeezed light from lasers with sharply nonlinear gain at optical frequencies, Phys. Rev. Lett. **131**, 173801 (2023).

[41] J. F. Tasker, J. Frazer, G. Ferranti, E. J. Allen, L. F. Brunel, S. Tanzilli, V. D'Auria, and J. C. F. Matthews, Silicon photonics interfaced with integrated electronics for 9 GHz measurement of squeezed light, Nat. Photon. **15**, 11 (2021).

[42] E. Waks, C. Santori, and Y. Yamamoto, Security aspects of quantum key distribution with sub-Poisson light, Phys. Rev. A **66**, 042315 (2002).

[43] C. S. Jacobsen, L. S. Madsen, V. C. Usenko, R. Filip, and U. L. Andersen, Complete elimination of information leakage in continuous-variable quantum communication channels, npj Quantum Inf. **4**, 32 (2018).

[44] I. Derkach, V. C. Usenko, and R. Filip, Squeezing-enhanced quantum key distribution over atmospheric channels, New J. Phys. **22**, 053006 (2020).

[45] N. Hosseinidehaj, M. S. Winnel, and T. C. Ralph, Simple and loss-tolerant free-space quantum key distribution using a squeezed laser, Phys. Rev. A **105**, 032602 (2022).

[46] D. Soh and E. Chatterjee, Label-free quantum super-resolution imaging using entangled multi-mode squeezed light, New J. Phys. **25**, 093001 (2023).